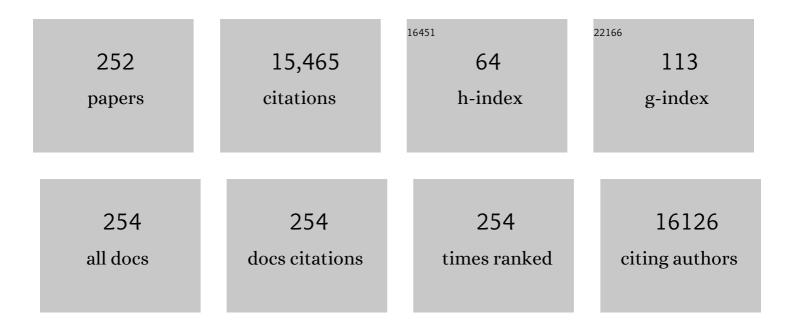
Jian-Sheng Jie

List of Publications by Year in descending order

Source: https://exaly.com/author-pdf/3463408/publications.pdf Version: 2024-02-01



INN-SHENC LE

#	Article	IF	CITATIONS
1	Organic Semiconductor Crystal Engineering for Highâ€Resolution Layerâ€Controlled 2D Crystal Arrays. Advanced Materials, 2022, 34, e2104166.	21.0	18
2	Ambient instability of organic field-effect transistors and their improvement strategies. Journal Physics D: Applied Physics, 2022, 55, 053001.	2.8	8
3	Applying intermolecular hydrogen bonding to exploit TADF emitters for high-performance orange-red non-doped OLEDs. Journal of Materials Chemistry C, 2022, 10, 4717-4722.	5.5	7
4	Conformal MoS ₂ /Silicon Nanowire Array Heterojunction with Enhanced Light Trapping and Effective Interface Passivation for Ultraweak Infrared Light Detection. Advanced Functional Materials, 2022, 32, 2108174.	14.9	32
5	Scalable Growth of Organic Singleâ€Crystal Films via an Orientation Filter Funnel for Highâ€Performance Transistors with Excellent Uniformity. Advanced Materials, 2022, 34, e2109818.	21.0	29
6	Wafer-Scale Fabrication of Silicon Nanocones via Controlling Catalyst Evolution in All-Wet Metal-Assisted Chemical Etching. ACS Omega, 2022, 7, 2234-2243.	3.5	7
7	Soft template-assisted self-assembly: a general strategy toward two-dimensional molecular crystals for high-performance organic field-effect transistors. Journal of Materials Chemistry C, 2022, 10, 2575-2580.	5.5	5
8	Enhancing the efficiency and stability of Organic/Silicon solar cells using graphene electrode and Double-layer Anti-reflection coating. Solar Energy, 2022, 234, 111-118.	6.1	13
9	<i>In Situ</i> Fabrication of PdSe ₂ /GaN Schottky Junction for Polarization-Sensitive Ultraviolet Photodetection with High Dichroic Ratio. ACS Nano, 2022, 16, 5545-5555.	14.6	139
10	A Fully Solutionâ€Printed Photosynaptic Transistor Array with Ultralow Energy Consumption for Artificialâ€Vision Neural Networks. Advanced Materials, 2022, 34, e2200380.	21.0	75
11	A Threeâ€Dimensional Confined Crystallization Strategy Toward Controllable Growth of Highâ€Quality and Largeâ€Area Perovskite Single Crystals. Advanced Functional Materials, 2022, 32, .	14.9	17
12	High-Luminance Microsized CH ₃ NH ₃ PbBr ₃ Single-Crystal-Based Light-Emitting Diodes via a Facile Liquid-Insulator Bridging Route. ACS Nano, 2022, 16, 6394-6403.	14.6	13
13	Ultraâ€5ensitive and Lowâ€Powerâ€Consumption Organic Phototransistor Enables Nighttime Illumination Perception for Bionic Mesopic Vision. Laser and Photonics Reviews, 2022, 16, .	8.7	10
14	Highâ€Barrierâ€Height Ti ₃ C ₂ T <i>_x</i> /Si Microstructure Schottky Junctionâ€Based Selfâ€Powered Photodetectors for Photoplethysmographic Monitoring. Advanced Materials Technologies, 2022, 7, .	5.8	15
15	Insights into the Origins of Minority Carrier Traps in Solutionâ€Processed Organic Semiconductors and Their Effects on Transistor Photostability. Advanced Electronic Materials, 2022, 8, .	5.1	5
16	Waterâ€Surface Drag Coating: A New Route Toward Highâ€Quality Conjugated Smallâ€Molecule Thin Films with Enhanced Charge Transport Properties. Advanced Materials, 2021, 33, e2005915.	21.0	52
17	Solution-Processable Carbon and Graphene Quantum Dots Photodetectors. Lecture Notes in Nanoscale Science and Technology, 2021, , 157-214.	0.8	1
18	2D molecular crystal templated organic p–n heterojunctions for high-performance ambipolar organic field-effect transistors. Journal of Materials Chemistry C, 2021, 9, 5758-5764.	5.5	12

#	Article	IF	CITATIONS
19	Precise patterning of single crystal arrays of organic semiconductors by a patterned microchannel dip-coating method for organic field-effect transistors. Journal of Materials Chemistry C, 2021, 9, 5174-5181.	5.5	10
20	Improving Ideality of Pâ€Type Organic Fieldâ€Effect Transistors via Preventing Undesired Minority Carrier Injection. Advanced Functional Materials, 2021, 31, 2100202.	14.9	21
21	Patterning Liquid Crystalline Organic Semiconductors via Inkjet Printing for Highâ€Performance Transistor Arrays and Circuits. Advanced Functional Materials, 2021, 31, 2100237.	14.9	57
22	Highâ€Performance Nondoped Organic Lightâ€Emitting Diode Based on a Thermally Activated Delayed Fluorescence Emitter with 1D Intermolecular Hydrogen Bonding Interactions. Advanced Optical Materials, 2021, 9, 2100461.	7.3	16
23	Ultrabroadband and High-Detectivity Photodetector Based on WS ₂ /Ge Heterojunction through Defect Engineering and Interface Passivation. ACS Nano, 2021, 15, 10119-10129.	14.6	252
24	Singleâ€Crystalline Silicon Frameworks: A New Platform for Transparent Flexible Optoelectronics. Advanced Materials, 2021, 33, e2008171.	21.0	13
25	A phototransistor with visual adaptation. Nature Electronics, 2021, 4, 460-461.	26.0	4
26	Characterizing the Conformational Distribution in an Amorphous Film of an Organic Emitter and Its Application in a "Selfâ€Đoping―Organic Lightâ€Emitting Diode. Angewandte Chemie, 2021, 133, 26082-260)87.	8
27	Waferâ€Scale Growth of Aligned C ₆₀ Single Crystals via Solutionâ€Phase Epitaxy for Highâ€Performance Transistors. Advanced Functional Materials, 2021, 31, 2105459.	14.9	9
28	Characterizing the Conformational Distribution in an Amorphous Film of an Organic Emitter and Its Application in a "Selfâ€Đoping―Organic Lightâ€Emitting Diode. Angewandte Chemie - International Edition, 2021, 60, 25878-25883.	13.8	35
29	Bilayer-passivated stable dif-TES-ADT organic thin-film transistors. Applied Physics Letters, 2021, 119, 183301.	3.3	4
30	Roles of interfaces in the ideality of organic field-effect transistors. Nanoscale Horizons, 2020, 5, 454-472.	8.0	25
31	Cation exchange synthesis of two-dimensional vertical Cu ₂ S/CdS heterojunctions for photovoltaic device applications. Journal of Materials Chemistry A, 2020, 8, 789-796.	10.3	23
32	Theoretical Studies of Bipolar Transport in CnBTBT–FmTCNQ Donor–Acceptor Cocrystals. Journal of Physical Chemistry Letters, 2020, 11, 359-365.	4.6	15
33	Surficial Marangoni Flowâ€Induced Growth of Ultrathin 2D Molecular Crystals on Target Substrates. Advanced Materials Interfaces, 2020, 7, 1901753.	3.7	10
34	Ultrahigh Speed and Broadband Few‣ayer MoTe ₂ /Si 2D–3D Heterojunctionâ€Based Photodiodes Fabricated by Pulsed Laser Deposition. Advanced Functional Materials, 2020, 30, 1907951.	14.9	119
35	High-resolution patterning of organic semiconductor single crystal arrays for high-integration organic field-effect transistors. Materials Today, 2020, 40, 82-90.	14.2	53
36	Atomic-Scale Interface Engineering for Constructing p-CuPc/n-CdS Core–Shell Heterojunctions toward Light-Harvesting Application. ACS Applied Energy Materials, 2020, 3, 8765-8773.	5.1	2

#	Article	IF	CITATIONS
37	Hydrogen bond-modulated molecular packing and its applications in high-performance non-doped organic electroluminescence. Materials Horizons, 2020, 7, 2734-2740.	12.2	51
38	Grapheneâ€Quantumâ€Dotsâ€Induced Centimeterâ€Sized Growth of Monolayer Organic Crystals for Highâ€Performance Transistors. Advanced Materials, 2020, 32, e2003315.	21.0	27
39	Van der Waals Epitaxial Growth of Mosaicâ€Like 2D Platinum Ditelluride Layers for Roomâ€Temperature Midâ€Infrared Photodetection up to 10.6 µm. Advanced Materials, 2020, 32, e2004412.	21.0	202
40	Fast deposition of an ultrathin, highly crystalline organic semiconductor film for high-performance transistors. Nanoscale Horizons, 2020, 5, 1096-1105.	8.0	20
41	Few‣ayer Organic Crystalline van der Waals Heterojunctions for Ultrafast UV Phototransistors. Advanced Electronic Materials, 2020, 6, 2000062.	5.1	22
42	Ultraminiaturized Stretchable Strain Sensors Based on Single Silicon Nanowires for Imperceptible Electronic Skins. Nano Letters, 2020, 20, 2478-2485.	9.1	51
43	A Microchannelâ€Confined Crystallization Strategy Enables Blade Coating of Perovskite Single Crystal Arrays for Device Integration. Advanced Materials, 2020, 32, e1908340.	21.0	75
44	Meniscus-guided coating of organic crystalline thin films for high-performance organic field-effect transistors. Journal of Materials Chemistry C, 2020, 8, 9133-9146.	5.5	49
45	Controlled 2D growth of organic semiconductor crystals by suppressing "coffee-ring―effect. Nano Research, 2020, 13, 2478-2484.	10.4	11
46	An ultrasensitive self-driven broadband photodetector based on a 2D-WS ₂ /GaAs type-II Zener heterojunction. Nanoscale, 2020, 12, 4435-4444.	5.6	56
47	Mixed-dimensional PdSe ₂ /SiNWA heterostructure based photovoltaic detectors for self-driven, broadband photodetection, infrared imaging and humidity sensing. Journal of Materials Chemistry A, 2020, 8, 3632-3642.	10.3	158
48	Channel-restricted meniscus self-assembly for uniformly aligned growth of single-crystal arrays of organic semiconductors. Materials Today, 2019, 24, 17-25.	14.2	98
49	Layerâ€Defining Strategy to Grow Twoâ€Dimensional Molecular Crystals on a Liquid Surface down to the Monolayer Limit. Angewandte Chemie - International Edition, 2019, 58, 16082-16086.	13.8	53
50	2D Ruddlesden–Popper Perovskite Nanoplate Based Deepâ€Blue Lightâ€Emitting Diodes for Light Communication. Advanced Functional Materials, 2019, 29, 1903861.	14.9	101
51	Highly Polarization-Sensitive, Broadband, Self-Powered Photodetector Based on Graphene/PdSe ₂ /Germanium Heterojunction. ACS Nano, 2019, 13, 9907-9917.	14.6	420
52	Unraveling the Mechanism of the Persistent Photoconductivity in Organic Phototransistors. Advanced Functional Materials, 2019, 29, 1905657.	14.9	54
53	Air Effect on the Ideality of pâ€Type Organic Fieldâ€Effect Transistors: A Doubleâ€Edged Sword. Advanced Functional Materials, 2019, 29, 1906653.	14.9	25
54	Precise Positioning of Organic Semiconductor Single Crystals with Two-Component Aligned Structure through 3D Wettability-Induced Sequential Assembly. ACS Applied Materials & Interfaces, 2019, 11, 36205-36212.	8.0	17

#	Article	IF	CITATIONS
55	One-step growth of large-area silicon nanowire fabrics for high-performance multifunctional wearable sensors. Nano Research, 2019, 12, 2723-2728.	10.4	11
56	External-force-driven solution epitaxy of large-area 2D organic single crystals for high-performance field-effect transistors. Nano Research, 2019, 12, 2796-2801.	10.4	26
57	Quantum transport characteristics of heavily doped bismuth selenide nanoribbons. Npj Quantum Materials, 2019, 4, .	5.2	40
58	Tuning Electrical and Raman Scattering Properties of Cadmium Sulfide Nanoribbons via Surface Charge Transfer Doping. Journal of Physical Chemistry C, 2019, 123, 15794-15801.	3.1	7
59	A Facile Method for the Growth of Organic Semiconductor Single Crystal Arrays on Polymer Dielectric toward Flexible Fieldâ€Effect Transistors. Advanced Functional Materials, 2019, 29, 1902494.	14.9	54
60	High-Performance Nanofloating Gate Memory Based on Lead Halide Perovskite Nanocrystals. ACS Applied Materials & Interfaces, 2019, 11, 24367-24376.	8.0	23
61	Dual-Band, High-Performance Phototransistors from Hybrid Perovskite and Organic Crystal Array for Secure Communication Applications. ACS Nano, 2019, 13, 5910-5919.	14.6	72
62	Precise Patterning of Organic Semiconductor Crystals for Integrated Device Applications. Small, 2019, 15, e1900332.	10.0	41
63	Memory phototransistors based on exponential-association photoelectric conversion law. Nature Communications, 2019, 10, 1294.	12.8	47
64	Photodetectors based on small-molecule organic semiconductor crystals. Chinese Physics B, 2019, 28, 038102.	1.4	16
65	Application of Silicon Oxide on High Efficiency Monocrystalline Silicon PERC Solar Cells. Energies, 2019, 12, 1168.	3.1	19
66	The Impact of Thermal Treatment on Light-Induced Degradation of Multicrystalline Silicon PERC Solar Cell. Energies, 2019, 12, 416.	3.1	14
67	Organic molecular crystal-based photosynaptic devices for an artificial visual-perception system. NPG Asia Materials, 2019, 11, .	7.9	81
68	Few-layer formamidinium lead bromide nanoplatelets for ultrapure-green and high-efficiency light-emitting diodes. Nano Research, 2019, 12, 171-176.	10.4	34
69	Saturated Vapor-Assisted Growth of Single-Crystalline Organic–Inorganic Hybrid Perovskite Nanowires for High-Performance Photodetectors with Robust Stability. ACS Applied Materials & Interfaces, 2018, 10, 10287-10295.	8.0	49
70	Organic–inorganic hybrid perovskite quantum dots for light-emitting diodes. Journal of Materials Chemistry C, 2018, 6, 4831-4841.	5.5	62
71	Tuning the electronic transport anisotropy in α -phase phosphorene through superlattice design. Physical Review B, 2018, 97, .	3.2	11
72	Hue tunable, high color saturation and high-efficiency graphene/silicon heterojunction solar cells with MgF2/ZnS double anti-reflection layer. Nano Energy, 2018, 46, 257-265.	16.0	51

#	Article	IF	CITATIONS
73	CdS Nanoribbonâ€Based Resistive Switches with Ultrawidely Tunable Power by Surface Charge Transfer Doping. Advanced Functional Materials, 2018, 28, 1706577.	14.9	16
74	Facile Assembly of Highâ€Quality Organic–Inorganic Hybrid Perovskite Quantum Dot Thin Films for Bright Lightâ€Emitting Diodes. Advanced Functional Materials, 2018, 28, 1705189.	14.9	52
75	Integrated MoSe2 with n+p-Si photocathodes for solar water splitting with high efficiency and stability. Applied Physics Letters, 2018, 112, .	3.3	30
76	Advanced interface modelling of n-Si/HNO3 doped graphene solar cells to identify pathways to high efficiency. Applied Surface Science, 2018, 434, 102-111.	6.1	10
77	ZnSe nanoribbon-Si nanowire crossed p-n nano-heterojunctions: Electrical characterizations and photovoltaic applications. Solar Energy Materials and Solar Cells, 2018, 176, 411-417.	6.2	2
78	Flexible integrated diode-transistor logic (DTL) driving circuits based on printed carbon nanotube thin film transistors with low operation voltage. Nanoscale, 2018, 10, 614-622.	5.6	23
79	High-mobility air-stable n-type field-effect transistors based on large-area solution-processed organic single-crystal arrays. Nano Research, 2018, 11, 882-891.	10.4	25
80	Graphene/MoS ₂ /Si Nanowires Schottky-NP Bipolar van der Waals Heterojunction for Ultrafast Photodetectors. IEEE Electron Device Letters, 2018, 39, 1688-1691.	3.9	21
81	Precise Patterning of Laterally Stacked Organic Microbelt Heterojunction Arrays by Surfaceâ€Energyâ€Controlled Stepwise Crystallization for Ambipolar Organic Fieldâ€Effect Transistors. Advanced Materials, 2018, 30, e1800187.	21.0	56
82	Solutionâ€Processed 3D RGO–MoS ₂ /Pyramid Si Heterojunction for Ultrahigh Detectivity and Ultraâ€Broadband Photodetection. Advanced Materials, 2018, 30, e1801729.	21.0	175
83	1D Organic–Inorganic Hybrid Perovskite Micro/Nanocrystals: Fabrication, Assembly, and Optoelectronic Applications. Small Methods, 2018, 2, 1700340.	8.6	27
84	Light-trapping enhanced ZnO–MoS ₂ core–shell nanopillar arrays for broadband ultraviolet-visible-near infrared photodetection. Journal of Materials Chemistry C, 2018, 6, 7077-7084.	5.5	52
85	Efficient photovoltaic devices based on p-ZnSe/n-CdS core–shell heterojunctions with high open-circuit voltage. Journal of Materials Chemistry C, 2017, 5, 2107-2113.	5.5	12
86	Efficient and Stable Silicon Photocathodes Coated with Vertically Standing Nano-MoS ₂ Films for Solar Hydrogen Production. ACS Applied Materials & Interfaces, 2017, 9, 6123-6129.	8.0	96
87	Ultrahigh-Responsivity Photodetectors from Perovskite Nanowire Arrays for Sequentially Tunable Spectral Measurement. Nano Letters, 2017, 17, 2482-2489.	9.1	242
88	Metal Acetylacetonate Series in Interface Engineering for Full Lowâ€Temperatureâ€Processed, Highâ€Performance, and Stable Planar Perovskite Solar Cells with Conversion Efficiency over 16% on 1 cm ² Scale. Advanced Materials, 2017, 29, 1603923.	21.0	190
89	Ordered and Patterned Assembly of Organic Micro/Nanocrystals for Flexible Electronic and Optoelectronic Devices. Advanced Materials Technologies, 2017, 2, 1600280.	5.8	21
90	Precise Patterning of Organic Single Crystals via Capillaryâ€Assisted Alternatingâ€Electric Field. Small, 2017, 13, 1604261.	10.0	18

#	Article	IF	CITATIONS
91	One-step fabrication of CdS:Mo–CdMoO4core–shell nanoribbons for nonvolatile memory devices with high resistance switching. Journal of Materials Chemistry C, 2017, 5, 6156-6162.	5.5	8
92	Self-driven, broadband and ultrafast photovoltaic detectors based on topological crystalline insulator SnTe/Si heterostructures. Journal of Materials Chemistry A, 2017, 5, 11171-11178.	10.3	40
93	12.35% efficient graphene quantum dots/silicon heterojunction solar cells using graphene transparent electrode. Nano Energy, 2017, 31, 359-366.	16.0	114
94	The way to high-performance single nanowire photodetectors: problems and prospects. Science China: Physics, Mechanics and Astronomy, 2017, 60, 1.	5.1	2
95	Large-Scale Fabrication of Silicon Nanowires for Solar Energy Applications. ACS Applied Materials & Interfaces, 2017, 9, 34527-34543.	8.0	45
96	Controlled Growth of Large-Area Aligned Single-Crystalline Organic Nanoribbon Arrays for Transistors and Light-Emitting Diodes Driving. Nano-Micro Letters, 2017, 9, 52.	27.0	21
97	Tuning the Electronic and Optical Properties of Monolayers As, Sb, and Bi via Surface Charge Transfer Doping. Journal of Physical Chemistry C, 2017, 121, 19530-19537.	3.1	35
98	Centimeter-Long Single-Crystalline Si Nanowires. Nano Letters, 2017, 17, 7323-7329.	9.1	29
99	Surface charge transfer doping induced inversion layer for high-performance graphene/silicon heterojunction solar cells. Journal of Materials Chemistry A, 2017, 5, 285-291.	10.3	52
100	Alignment and Patterning of Ordered Smallâ€Molecule Organic Semiconductor Microâ€INanocrystals for Device Applications. Advanced Materials, 2016, 28, 2475-2503.	21.0	129
101	Topological insulator Bi ₂ Se ₃ nanowire/Si heterostructure photodetectors with ultrahigh responsivity and broadband response. Journal of Materials Chemistry C, 2016, 4, 5648-5655.	5.5	44
102	A facile method for fabrication of highly integrated organic field-effect transistors on photoresist-unwettable insulators with remarkable stability. Organic Electronics, 2016, 34, 104-110.	2.6	4
103	High-Responsivity, High-Detectivity, Ultrafast Topological Insulator Bi ₂ Se ₃ /Silicon Heterostructure Broadband Photodetectors. ACS Nano, 2016, 10, 5113-5122.	14.6	300
104	Ultrafast, Broadband Photodetector Based on MoSe ₂ /Silicon Heterojunction with Vertically Standing Layered Structure Using Graphene as Transparent Electrode. Advanced Science, 2016, 3, 1600018.	11.2	210
105	Surface Charge Transfer Doping of Lowâ€Dimensional Nanostructures toward Highâ€Performance Nanodevices. Advanced Materials, 2016, 28, 10409-10442.	21.0	144
106	An Inherent Multifunctional Sellotape Substrate for Highâ€Performance Flexible and Wearable Organic Singleâ€Crystal Nanowire Arrayâ€Based Transistors. Advanced Electronic Materials, 2016, 2, 1600129.	5.1	8
107	Surface Charge Transfer Doping <i>via</i> Transition Metal Oxides for Efficient p-Type Doping of Il–VI Nanostructures. ACS Nano, 2016, 10, 10283-10293.	14.6	31
108	Organometal Halide Perovskite Quantum Dot Lightâ€Emitting Diodes. Advanced Functional Materials, 2016, 26, 4797-4802.	14.9	231

#	Article	IF	CITATIONS
109	High-sensitivity and self-driven photodetectors based on Ge–CdS core–shell heterojunction nanowires via atomic layer deposition. CrystEngComm, 2016, 18, 3919-3924.	2.6	18
110	Length-dependent thermal transport in one-dimensional self-assembly of planar π-conjugated molecules. Nanoscale, 2016, 8, 11932-11939.	5.6	7
111	On the Mechanism of Hydrophilicity of Graphene. Nano Letters, 2016, 16, 4447-4453.	9.1	148
112	Aligned Singleâ€Crystalline Perovskite Microwire Arrays for Highâ€Performance Flexible Image Sensors with Longâ€Term Stability. Advanced Materials, 2016, 28, 2201-2208.	21.0	346
113	Two-dimensional layered material/silicon heterojunctions for energy and optoelectronic applications. Nano Research, 2016, 9, 72-93.	10.4	62
114	Bismuth-catalyzed and doped p-type ZnSe nanowires and their temperature-dependent charge transport properties. Journal of Materials Chemistry C, 2016, 4, 857-862.	5.5	4
115	Precisely Patterned Growth of Ultra-Long Single-Crystalline Organic Microwire Arrays for Near-Infrared Photodetectors. ACS Applied Materials & Interfaces, 2016, 8, 7912-7918.	8.0	26
116	Waferâ€5cale Precise Patterning of Organic Singleâ€Crystal Nanowire Arrays via a Photolithographyâ€Assisted Spinâ€Coating Method. Advanced Materials, 2015, 27, 7305-7312.	21.0	84
117	P- and N-type Surface Charge Transfer Doping of II-VI Group Semiconductor Nanostructures and Their Enhanced Optoelectronic Properties. , 2015, , .		0
118	Surface charge transfer induced p-CdS nanoribbon/n-Si heterojunctions as fast-speed self-driven photodetectors. Journal of Materials Chemistry C, 2015, 3, 6307-6313.	5.5	24
119	Flexible graphene/silicon heterojunction solar cells. Journal of Materials Chemistry A, 2015, 3, 14370-14377.	10.3	74
120	A solution-phase approach to Cd ₃ P ₂ nanowires: synthesis and characterization. Chemical Communications, 2015, 51, 2593-2596.	4.1	3
121	Facile One-Step Fabrication of Ordered Ultra-Long Organic Microwires Film for Flexible Near-Infrared Photodetectors. Journal of Nanoscience and Nanotechnology, 2015, 15, 4450-4456.	0.9	7
122	Organic Nanowire/Crystalline Silicon <i>p</i> – <i>n</i> Heterojunctions for High-Sensitivity, Broadband Photodetectors. ACS Applied Materials & Interfaces, 2015, 7, 2039-2045.	8.0	43
123	Solution-Processed Graphene Quantum Dot Deep-UV Photodetectors. ACS Nano, 2015, 9, 1561-1570.	14.6	249
124	Shape and composition control of Bi ₁₉ S ₂₇ (Br _{3â^'x} ,I _x) alloyed nanowires: the role of metal ions. Chemical Science, 2015, 6, 4615-4622.	7.4	24
125	Patterned growth of single-crystal 3, 4, 9, 10-perylenetetracarboxylic dianhydride nanowire arrays for field-emission and optoelectronic devices. Nanotechnology, 2015, 26, 295302.	2.6	4
126	MoO ₃ Nanodots Decorated CdS Nanoribbons for High-Performance, Homojunction Photovoltaic Devices on Flexible Substrates. Nano Letters, 2015, 15, 3590-3596.	9.1	38

#	Article	IF	CITATIONS
127	Bilayer graphene based surface passivation enhanced nano structured self-powered near-infrared photodetector. Optics Express, 2015, 23, 4839.	3.4	39
128	MoS ₂ /Si Heterojunction with Vertically Standing Layered Structure for Ultrafast, Highâ€Detectivity, Selfâ€Driven Visible–Near Infrared Photodetectors. Advanced Functional Materials, 2015, 25, 2910-2919.	14.9	554
129	Macroscopic and Strong Ribbons of Functionality-Rich Metal Oxides from Highly Ordered Assembly of Unilamellar Sheets. Journal of the American Chemical Society, 2015, 137, 13200-13208.	13.7	32
130	Surface Charge Transfer Doping of Monolayer Phosphorene via Molecular Adsorption. Journal of Physical Chemistry Letters, 2015, 6, 4701-4710.	4.6	63
131	Interfacial state induced ultrasensitive ultraviolet light photodetector with resolved flux down to 85 photons per second. Nano Research, 2015, 8, 1098-1107.	10.4	17
132	Smart Nanorods for Highly Effective Cancer Theranostic Applications. Advanced Healthcare Materials, 2014, 3, 906-915.	7.6	14
133	Very facile fabrication of aligned organic nanowires based high-performance top-gate transistors on flexible, transparent substrate. Organic Electronics, 2014, 15, 1317-1323.	2.6	23
134	Highly luminescent and photostable core–shell dye nanoparticles for high efficiency bioimaging. Chemical Communications, 2014, 50, 737-739.	4.1	17
135	Clean surface transfer of graphene films via an effective sandwich method for organic light-emitting diode applications. Journal of Materials Chemistry C, 2014, 2, 201-207.	5.5	55
136	Aligned nanowire arrays on thin flexible substrates for organic transistors with high bending stability. Journal of Materials Chemistry C, 2014, 2, 1314-1320.	5.5	36
137	Functional Core/Shell Drug Nanoparticles for Highly Effective Synergistic Cancer Therapy. Advanced Healthcare Materials, 2014, 3, 1475-1485.	7.6	22
138	Surface plasmon resonance enhanced highly efficient planar silicon solar cell. Nano Energy, 2014, 9, 112-120.	16.0	83
139	Large-Scale Assembly of Organic Micro/Nanocrystals into Highly Ordered Patterns and Their Applications for Strain Sensors. ACS Applied Materials & Interfaces, 2014, 6, 11018-11024.	8.0	18
140	Air Heating Approach for Multilayer Etching and Roll-to-Roll Transfer of Silicon Nanowire Arrays as SERS Substrates for High Sensitivity Molecule Detection. ACS Applied Materials & Interfaces, 2014, 6, 977-984.	8.0	18
141	Crystalline Si/Graphene Quantum Dots Heterojunction Solar Cells. Journal of Physical Chemistry C, 2014, 118, 5164-5171.	3.1	125
142	Interfacially Engineered Highâ€Speed Nonvolatile Memories Employing pâ€Type Nanoribbons. Advanced Materials Interfaces, 2014, 1, 1400130.	3.7	3
143	A High-yield Two-step Transfer Printing Method for Large-scale Fabrication of Organic Single-crystal Devices on Arbitrary Substrates. Scientific Reports, 2014, 4, 5358.	3.3	25
144	High-efficiency graphene/Si nanoarray Schottky junction solar cells via surface modification and graphene doping. Journal of Materials Chemistry A, 2013, 1, 6593.	10.3	122

#	Article	IF	CITATIONS
145	In Situ Integration of Squaraine-Nanowire-Array-Based Schottky-Type Photodetectors with Enhanced Switching Performance. ACS Applied Materials & Interfaces, 2013, 5, 12288-12294.	8.0	30
146	Ultralow Contact Resistivity of Cu/Au With \$p\$-Type ZnS Nanoribbons for Nanoelectronic Applications. IEEE Electron Device Letters, 2013, 34, 810-812.	3.9	8
147	Large-area aligned growth of single-crystalline organic nanowire arrays for high-performance photodetectors. Nanotechnology, 2013, 24, 355201.	2.6	35
148	CTAB Assisted Synthesis of CuS Microcrystals: Synthesis, Mechanism, and Electrical Properties. Journal of Materials Science and Technology, 2013, 29, 1047-1052.	10.7	31
149	The application of single-layer graphene modified with solution-processed TiOx and PEDOT:PSS as a transparent conductive anode in organic light-emitting diodes. Organic Electronics, 2013, 14, 3348-3354.	2.6	41
150	High-Sensitivity and Fast-Response Graphene/Crystalline Silicon Schottky Junction-Based Near-IR Photodetectors. IEEE Electron Device Letters, 2013, 34, 1337-1339.	3.9	136
151	Large conductance switching nonvolatile memories based on p-ZnS nanoribbon/n-Si heterojunction. Journal of Materials Chemistry C, 2013, 1, 1238-1244.	5.5	10
152	Large-scale assembly of semiconductor nanowires into desired patterns for sensor applications. New Journal of Chemistry, 2013, 37, 1776.	2.8	6
153	Hole-induced large-area homoepitaxial growth of CdSe nanowire arrays for photovoltaic application. Journal of Materials Chemistry A, 2013, 1, 6313.	10.3	6
154	High-efficiency, air stable graphene/Si micro-hole array Schottky junction solar cells. Journal of Materials Chemistry A, 2013, 1, 15348.	10.3	86
155	Shape design of high drug payload nanoparticles for more effective cancer therapy. Chemical Communications, 2013, 49, 10989.	4.1	47
156	Tuning the p-type conductivity of ZnSe nanowiresvia silver doping for rectifying and photovoltaic device applications. Journal of Materials Chemistry A, 2013, 1, 1148-1154.	10.3	29
157	Carrier-free functionalized multidrug nanorods for synergistic cancer therapy. Biomaterials, 2013, 34, 8960-8967.	11.4	104
158	Flexible CuS nanotubes–ITO film Schottky junction solar cells with enhanced light harvesting by using an Ag mirror. Nanotechnology, 2013, 24, 045402.	2.6	16
159	Monolayer Graphene Film on ZnO Nanorod Array for Highâ€Performance Schottky Junction Ultraviolet Photodetectors. Small, 2013, 9, 2872-2879.	10.0	271
160	Graphene Transparent Conductive Electrodes for Highly Efficient Silicon Nanostructures-Based Hybrid Heterojunction Solar Cells. Journal of Physical Chemistry C, 2013, 117, 11968-11976.	3.1	96
161	Surface passivation and band engineering: a way toward high efficiency graphene–planar Si solar cells. Journal of Materials Chemistry A, 2013, 1, 8567.	10.3	123
162	Fabrication of p-type ZnSe:Sb nanowires for high-performance ultraviolet light photodetector application. Nanotechnology, 2013, 24, 095603.	2.6	36

#	Article	IF	CITATIONS
163	Self-Assembly and Hierarchical Patterning of Aligned Organic Nanowire Arrays by Solvent Evaporation on Substrates with Patterned Wettability. ACS Applied Materials & Interfaces, 2013, 5, 5757-5762.	8.0	29
164	Ultrahigh Mobility of pâ€Type CdS Nanowires: Surface Charge Transfer Doping and Photovoltaic Devices. Advanced Energy Materials, 2013, 3, 579-583.	19.5	37
165	ZnSe nanowire/Si p–n heterojunctions: device construction and optoelectronic applications. Nanotechnology, 2013, 24, 395201.	2.6	33
166	In-situ device integration of large-area patterned organic nanowire arrays for high-performance optical sensors. Scientific Reports, 2013, 3, 3248.	3.3	25
167	ZnSe nanoribbon/Si nanowire p–n heterojunction arrays and their photovoltaic application with graphene transparent electrodes. Journal of Materials Chemistry, 2012, 22, 22873.	6.7	32
168	Surface charge transfer doping of germanium nanowires by MoO3 deposition. RSC Advances, 2012, 2, 3361.	3.6	7
169	Transparent and flexible selenium nanobelt-based visible light photodetector. CrystEngComm, 2012, 14, 1942.	2.6	68
170	Nonvolatile multibit Schottky memory based on single n-type Ga doped CdSe nanowires. Nanotechnology, 2012, 23, 485203.	2.6	15
171	Device structure-dependent field-effect and photoresponse performances of p-type ZnTe:Sb nanoribbons. Journal of Materials Chemistry, 2012, 22, 6206.	6.7	96
172	p-CdTe nanoribbon/n-silicon nanowires array heterojunctions: photovoltaic devices and zero-power photodetectors. CrystEngComm, 2012, 14, 7222.	2.6	38
173	Aligned ultralong nanowire arrays and their application in flexible photodetector devices. Journal of Materials Chemistry, 2012, 22, 14357.	6.7	46
174	Highly branched organic microcrystals via self-organization and growth kinetics manipulation. CrystEngComm, 2012, 14, 8124.	2.6	16
175	Facile formation of microscale hollow superstructures made of organic nanocrystals and their application as a humidity sensor. CrystEngComm, 2012, 14, 819-823.	2.6	7
176	Aluminium-doped n-type ZnS nanowires as high-performance UV and humidity sensors. Journal of Materials Chemistry, 2012, 22, 6856.	6.7	79
177	Schottky solar cells based on graphene nanoribbon/multiple silicon nanowires junctions. Applied Physics Letters, 2012, 100, 193103.	3.3	65
178	Chlorineâ€Doped ZnSe Nanoribbons with Tunable nâ€Type Conductivity as Highâ€Gain and Flexible Blue/UV Photodetectors. ChemPlusChem, 2012, 77, 470-475.	2.8	15
179	Tailoring the electrical properties of tellurium nanowires via surface charge transfer doping. Journal of Nanoparticle Research, 2012, 14, 1.	1.9	13
180	Composition tuning of room-temperature nanolasers. Vacuum, 2012, 86, 737-741.	3.5	13

#	Article	IF	CITATIONS
181	Largeâ€Scale Controllable Patterning Growth of Aligned Organic Nanowires through Evaporationâ€Induced Selfâ€Assembly. Chemistry - A European Journal, 2012, 18, 975-980.	3.3	18
182	Synthesis of Sb-Doped <i>p</i> -Type CdTe Nanowires and Their Application as High-Performance Nano-Schottky Barrier Diodes. Journal of Nanoengineering and Nanomanufacturing, 2012, 2, 191-196.	0.3	8
183	High-Performance Blue-Light Photodetectors Based on Single-Crystal ZnSe Nanoribbons with Controlled Gallium Doping. Science of Advanced Materials, 2012, 4, 332-336.	0.7	9
184	High-gain visible-blind UV photodetectors based on chlorine-doped n-type ZnS nanoribbons with tunable optoelectronic properties. Journal of Materials Chemistry, 2011, 21, 12632.	6.7	64
185	Tuning the electrical transport properties of n-type CdS nanowiresvia Ga doping and their nano-optoelectronic applications. Physical Chemistry Chemical Physics, 2011, 13, 14663.	2.8	47
186	Construction of high-quality CdS:Ga nanoribbon/silicon heterojunctions and their nano-optoelectronic applications. Nanotechnology, 2011, 22, 405201.	2.6	40
187	Surface Dangling Bond-Mediated Molecules Doping of Germanium Nanowires. Journal of Physical Chemistry C, 2011, 115, 24293-24299.	3.1	18
188	Monolayer graphene film/silicon nanowire array Schottky junction solar cells. Applied Physics Letters, 2011, 99, .	3.3	120
189	Surface induced negative photoconductivity in p-type ZnSe : Bi nanowires and their nano-optoelectronic applications. Journal of Materials Chemistry, 2011, 21, 6736.	6.7	89
190	Doping dependent crystal structures and optoelectronic properties of n-type CdSe:Ga nanowries. Nanoscale, 2011, 3, 4798.	5.6	27
191	Sn-catalyzed synthesis of SnO2nanowires and their optoelectronic characteristics. Nanotechnology, 2011, 22, 485701.	2.6	51
192	Single-crystalline ZnTe nanowires for application as high-performance Green/Ultraviolet photodetector. Optics Express, 2011, 19, 6100.	3.4	91
193	Structure and electrical properties of p-type twin ZnTe nanowires. Applied Physics A: Materials Science and Processing, 2011, 102, 469-475.	2.3	19
194	Synthesis and optoelectronic properties of silver-doped n-type CdS nanoribbons. Frontiers of Optoelectronics in China, 2011, 4, 161-165.	0.2	4
195	Nano-Schottky barrier diodes based on Sb-doped ZnS nanoribbons with controlled p-type conductivity. Applied Physics Letters, 2011, 98, .	3.3	35
196	Chlorine-doped n-type CdS nanowires with enhanced photoconductivity. Nanotechnology, 2011, 22, 069801.	2.6	2
197	Nitrogen Doped <i>n</i> -Type CdS Nanoribbons with Tunable Electrical and Photoelectrical Properties. Journal of Nanoscience and Nanotechnology, 2011, 11, 2003-2011.	0.9	4
198	One-dimensional II–VI nanostructures: Synthesis, properties and optoelectronic applications. Nano Today, 2010, 5, 313-336.	11.9	293

#	Article	IF	CITATIONS
199	High-performance CdS:P nanoribbon field-effect transistors constructed with high- \hat{I}^{2} dielectric and top-gate geometry. Applied Physics Letters, 2010, 96, .	3.3	41
200	Field Effect Properties of Phosphorus Doped CdS Single-Crystal Nanoribbon via Co-Thermal-Evaporation. Journal of Nanoscience and Nanotechnology, 2010, 10, 433-439.	0.9	10
201	Coaxial ZnSe/Si nanocables with controlled p-type shell doping. Nanotechnology, 2010, 21, 285206.	2.6	15
202	High-Performance CdSe:In Nanowire Field-Effect Transistors Based on Top-Gate Configuration with High-κ Non-Oxide Dielectrics. Journal of Physical Chemistry C, 2010, 114, 4663-4668.	3.1	21
203	Enhanced p-Type Conductivity of ZnTe Nanoribbons by Nitrogen Doping. Journal of Physical Chemistry C, 2010, 114, 7980-7985.	3.1	51
204	Chlorine-doped n-type CdS nanowires with enhanced photoconductivity. Nanotechnology, 2010, 21, 505203.	2.6	66
205	Green chemical approaches to ZnSe quantum dots: preparation, characterisation and formation mechanism. Journal of Experimental Nanoscience, 2010, 5, 106-117.	2.4	15
206	High-performance, fully transparent, and flexible zinc-doped indium oxide nanowire transistors. Applied Physics Letters, 2009, 94, .	3.3	46
207	Silicon nanowire sensors for Hg2+ and Cd2+ ions. Applied Physics Letters, 2009, 94, .	3.3	83
208	Phosphine-Free Synthesis of CdSe Quantum Dots in a New Co-CappingLigand System. Journal of Nanoscience and Nanotechnology, 2009, 9, 4735-4740.	0.9	9
209	Photoconductive Properties of Selenium Nanowire Photodetectors. Journal of Nanoscience and Nanotechnology, 2009, 9, 6292-6298.	0.9	26
210	Gallium-assisted growth of flute-like MgO nanotubes, Ga ₂ O ₃ -filled MgO nanotubes, and MgO/Ga ₂ O ₃ co-axial nanotubes. Nanotechnology, 2009, 20, 075602.	2.6	9
211	Facile Oneâ€Step Fabrication of Ordered Organic Nanowire Films. Advanced Materials, 2009, 21, 4172-4175.	21.0	68
212	Innentitelbild: Polyhedral Organic Microcrystals: From Cubes to Rhombic Dodecahedra (Angew. Chem.) Tj ETQqC	0 0 rgBT 2.0	/Oyerlock 10
213	Polyhedral Organic Microcrystals: From Cubes to Rhombic Dodecahedra. Angewandte Chemie - International Edition, 2009, 48, 9121-9123.	13.8	97
214	Inside Cover: Polyhedral Organic Microcrystals: From Cubes to Rhombic Dodecahedra (Angew. Chem.) Tj ETQq0	0 0 rgBT / 13.8	Overlock 10 ⁻
215	Tuning Electrical and Photoelectrical Properties of CdSe Nanowires via Indium Doping. Small, 2009, 5, 345-350.	10.0	78
216	Synthesis of CdSXSe1â^'X Nanoribbons with Uniform and Controllable Compositions via Sulfurization:	3.1	27

Optical and Electronic Properties Studies. Journal of Physical Chemistry C, 2009, 113, 17183-17188. 216

#	Article	IF	CITATIONS
217	Formation and Photoelectric Properties of Periodically Twinned ZnSe/SiO2 Nanocables. Journal of Physical Chemistry C, 2009, 113, 834-838.	3.1	42
218	Synthesis and Characterization of In-Doped ZnO Planar Superlattice Nanoribbons. Journal of Physical Chemistry C, 2009, 113, 5417-5421.	3.1	19
219	New strategy for the synthesis and characterization of monodisperse Zn7.23Cd2.77S10 nanoparticles. Journal of Alloys and Compounds, 2009, 481, 644-648.	5.5	9
220	Coaxial nanocables of p-type zinc telluride nanowires sheathed with silicon oxide: synthesis, characterization and properties. Nanotechnology, 2009, 20, 455702.	2.6	20
221	Tectonic arrangement of Bi2S3 nanocrystals into 2D networks. Journal of Materials Chemistry, 2009, 19, 3378.	6.7	38
222	Surfaceâ€Dominated Transport Properties of Silicon Nanowires. Advanced Functional Materials, 2008, 18, 3251-3257.	14.9	180
223	Tunable n‶ype Conductivity and Transport Properties of Gaâ€doped ZnO Nanowire Arrays. Advanced Materials, 2008, 20, 168-173.	21.0	203
224	Facile Oneâ€Step Growth and Patterning of Aligned Squaraine Nanowires via Evaporationâ€Induced Selfâ€Assembly. Advanced Materials, 2008, 20, 1716-1720.	21.0	123
225	Photoconductivity of a Single Smallâ€Molecule Organic Nanowire. Advanced Materials, 2008, 20, 2427-2432.	21.0	108
226	Preparation of Large-Area Uniform Silicon Nanowires Arrays through Metal-Assisted Chemical Etching. Journal of Physical Chemistry C, 2008, 112, 4444-4450.	3.1	504
227	p-Type ZnO Nanowire Arrays. Nano Letters, 2008, 8, 2591-2597.	9.1	237
228	Silicon nanowires for rechargeable lithium-ion battery anodes. Applied Physics Letters, 2008, 93, .	3.3	372
229	Millimeter-Long and Uniform Silicon Nanocables. Journal of Physical Chemistry C, 2008, 112, 15943-15947.	3.1	1
230	Single zinc-doped indium oxide nanowire as driving transistor for organic light-emitting diode. Applied Physics Letters, 2008, 92, .	3.3	29
231	Hysteresis in In2O3:Zn nanowire field-effect transistor and its application as a nonvolatile memory device. Applied Physics Letters, 2008, 93, 183111.	3.3	13
232	Applications of silicon nanowires functionalized with palladium nanoparticles in hydrogen sensors. Nanotechnology, 2007, 18, 345502.	2.6	74
233	Photoresponse Properties of CdSe Single-Nanoribbon Photodetectors. Advanced Functional Materials, 2007, 17, 1795-1800.	14.9	257
234	Photoconductive Characteristics of Single-Crystal CdS Nanoribbons. Nano Letters, 2006, 6, 1887-1892.	9.1	540

#	Article	IF	CITATIONS
235	Homoepitaxial Growth and Lasing Properties of ZnS Nanowire and Nanoribbon Arrays. Advanced Materials, 2006, 18, 1527-1532.	21.0	140
236	Heterocrystal and bicrystal structures of ZnS nanowires synthesized by plasma enhanced chemical vapour deposition. Nanotechnology, 2006, 17, 2913-2917.	2.6	24
237	Transport properties of single-crystal CdS nanoribbons. Applied Physics Letters, 2006, 89, 223117.	3.3	53
238	Single-crystal CdSe nanoribbon field-effect transistors and photoelectric applications. Applied Physics Letters, 2006, 89, 133118.	3.3	62
239	Optical properties of ZnO cone arrays and influence of annealing on optical properties of ZnO-Zn coaxial nanocables. , 2005, , .		1
240	Properties of Zn1â^'xCoxO thin films grown on silicon substrates prepared by pulsed laser deposition. Thin Solid Films, 2005, 491, 249-252.	1.8	15
241	Non-aqueous cathodic electrodeposition of large-scale uniform ZnO nanowire arrays embedded in anodic alumina membrane. Materials Letters, 2005, 59, 1378-1382.	2.6	44
242	Annealing effect on optical properties of ZnO films fabricated by cathodic electrodeposition. Thin Solid Films, 2005, 492, 61-65.	1.8	53
243	Preparation and optical properties of ZnO films by cathodic electrodeposition. , 2005, 5632, 226.		0
244	Controllable Synthesis and Optical Properties of Novel ZnO Cone Arrays via Vapor Transport at Low Temperature. Journal of Physical Chemistry B, 2005, 109, 2733-2738.	2.6	65
245	Synthesis and optical properties of well-aligned ZnO nanorod array on an undoped ZnO film. Applied Physics Letters, 2005, 86, 031909.	3.3	154
246	Growth and properties of well-aligned ZnO hexagonal cones prepared by carbonthermal reaction. Journal of Crystal Growth, 2004, 267, 223-230.	1.5	19
247	Indium-doped zinc oxide nanobelts. Chemical Physics Letters, 2004, 387, 466-470.	2.6	200
248	Synthesis and Characterization of ZnO:In Nanowires with Superlattice Structure. Journal of Physical Chemistry B, 2004, 108, 17027-17031.	2.6	95
249	Growth of Ternary Oxide Nanowires by Gold-Catalyzed Vapor-Phase Evaporation. Journal of Physical Chemistry B, 2004, 108, 8249-8253.	2.6	72
250	Synthesis and Characterization of Aligned ZnO Nanorods on Porous Aluminum Oxide Template. Journal of Physical Chemistry B, 2004, 108, 11976-11980.	2.6	102
251	Hole drilling of Inconel 718 by high intensity pulsed ultraviolet laser. Journal of Laser Applications, 2003, 15, 168-171.	1.7	5
252	Study of superalloy topography during ultrahigh intensity nanosecond ultraviolet laser ablation. Journal of Applied Physics, 2002, 91, 6761.	2.5	3